Proc. Natl. Acad. Sci. USA
Vol. 86, pp. 1505–1509, March 1989
Biophysics

Comparative study of optical absorption and circular dichroism of bacteriochlorophyll oligomers in Triton X-100, the antenna pigment B850, and the primary donor P-860 of photosynthetic bacteria indicates that all are similar dimers of bacteriochlorophyll *a*

(photosynthesis/light-harvesting complexes/chromophore–protein organization/exciton theory)

A. SCHERZ* AND V. ROSENBACH-BELKIN

Department of Biochemistry, The Weizmann Institute of Science, Rehovot 76100, Israel

Communicated by Joseph J. Katz, April 1, 1988

ABSTRACT **Dimers of bacteriochlorophyll a (Bchl*a*) with optical absorption maximum at 853 nm and a nonconservative circular dichroism spectrum are formed in a solution of formamide/water that contains micelles of Triton X-100. The apparent equilibrium constant and the corresponding Gibbs energy change for the Bchl self-organization are $4.9 \times 10^6\ M^{-1}$ and −9.2 kcal/mol, respectively. The experimental absorption and circular dichroism spectra of the *in vitro* Bchl dimer (termed Bchl-853) are similar to the spectra of the bacterial light-harvesting complex B850 and the primary electron donor P-860 and probably point to a common structural motif. Indeed, simulation of the dimers' spectra (optical absorption and circular dichroism), achieved by using an extended version of the exciton theory, suggests the same geometry as recently elucidated for P-860 by x-ray diffraction crystallography. The proposed geometry is predicted to have the minimum energy in the gas phase. In conclusion, the spectral properties of the bathochromically shifted forms of Bchl*a* are likely a result of strong dipolar interactions in self-organized structures of Bchls.**

Biological photosynthesis converts electromagnetic radiation into useful chemical energy by the joint action of "antennas" and "photoreaction centers" (1). The antennas need to have a large cross section for the prevailing light absorption, stability for prolonged illumination, and the ability to transfer the collected energy with minimum dissipation and within the lifetime of the photoexcited singlet state into the site of electron allocation (1).

The purple photosynthetic bacteria implement these principles by a special network of bacteriochlorophylls (Bchls), carotenoids, and polypeptide matrices termed light-harvesting complexes (LHCs) (2). Relative to their spectral properties as isolated monomers *in vitro*, the *in vivo* Bchls show a bathochromic shift of the Q_y transition (2, 3) accompanied by induced optical activity (4) and increased oscillator strength (4, 5). Variations in the Q_y shift of the Bchls are usually accompanied by some modifications in the polypeptide composition and characterize different LHCs (1, 6). Bacteria of the same class may share a common pool of LHCs but in different proportions. For example, the Rhodospirillaceae contain the LHCs B800–820, B800–850, B850, B870, and B890 (termed by the Q_y transition of their Bchls); however, *Rhodobacter sphaeroides* contains mainly B800–850 and some B870, whereas *Rhodospirillum rubrum* contains mainly B870 (1). The various LHCs are packed around the photoreaction centers in order of descending absorption wavelength. As energy migrates from pigments absorbing at shorter wavelengths to those absorbing at longer ones a mechanism for fast energy flow is established (2). This energy is trapped by the special pair of Bchls, which functions as the primary electron donor (P). P has Q_y transition at a comparable wavelength to the longest-wavelength transitions of the LHCs.

Besides being an essential feature of the photosynthetic apparatus, the variable Q_y shift has been used to probe the *in vivo* setting of Bchls and chlorophylls in the following three approaches. The first suggests ground-state interactions in large aggregates of Bchls *in vivo* accompanied by mild coupling of degenerate excited states (7–13). The second approach proposes specific interactions between the occluded Bchls and the protein side chains [e.g., interactions with charged amino residues (14) or Schiff base formation (15)] that result in modification of the chromophores (3, 16–20). Updated sequencing (21–23) and hydropathy plots (24) of polypeptides from several LHCs do not support this hypothesis (25). Besides, it is clear now that the comparable shift in the Q_y transition of P-860 is primarily induced by interactions between the Bchls that make up the special pair (26–32). A third approach suggests that the bacterial LHCs (i.e., B850) contain individual Bchl–polypeptide units that have Q_y transition at 780–800 nm. The Bchl–polypeptide units form dimers in which the Bchls are tightly packed and their excited states are so strongly coupled that the Q_y wavelength shifts to 852 nm (25, 33). Further oligomerization of the Bchl–polypeptide dimers into a complete LHC should result in a weak exciton coupling of the shifted Q_y transitions that introduces strong and conservative circular dichroism (CD) around 852 nm. Under these assumptions a unique geometry of a Bchl*a* dimer has been found for which the calculated absorption and CD in the UV–visible–near IR region are in agreement with the experimental spectra of B850. The calculated geometry is strikingly similar to the one which has the minimum energy upon self-dimerization of Bchls in the gas phase (34). Therefore, it seemed possible to isolate *in vitro* dimers of Bchl*a* with similar structural and spectral properties. By implementing a controlled procedure for the Bchl*a* dimerization we hoped to (*i*) follow the development of the CD and absorption patterns as Bchls gather into dimers and the dimers into higher aggregates and (*ii*) estimate the role of Bchl self-organization in the construction of the *in vivo* chromophore–protein complexes.

MATERIALS AND METHODS

Formamide and pyridine (Merck) were used with no further purification. Bchl*a* was extracted from lyophilized cells of *Rhodospirillum rubrum* and purified as described (5). Sample

The publication costs of this article were defrayed in part by page charge payment. This article must therefore be hereby marked "*advertisement*" in accordance with 18 U.S.C. §1734 solely to indicate this fact.

Abbreviations: Bchl, bacteriochlorophyll; LHC, light-harvesting complex; TX-100, Triton X-100; Fw, formamide/water, 3:1 (vol/vol).

*To whom reprint requests should be addressed.

purity was checked by TLC and reversed-phase HPLC (as in ref. 35). No impurities (e.g., 10-hydroxy-Bchl*a*) were detected.

Large oligomers of Bchl*a* with optical absorption at 860 nm were prepared under dim light conditions (26). Triton X-100 (TX-100) (Sigma) was either (*i*) added to the Bchl*a* by cosonicating a 3:1 (vol/vol) formamide/water solution (Fw) that contained Bchl*a* with an equal volume of Fw that contained Tx-100 or (*ii*) added to Bchl*a* in pyridine before the addition of formamide. There was no difference in the final spectra. The Bchl*a* was kept in pyridine at −18°C before the experiment. Changes in the absorbance before and after the spectrum was recorded were always <2%. We also extracted the Bchl*a* from the Fw solution into diethyl ether and measured its purity by HPLC. No more than 0.5% impurities (e.g., 10-hydroxy-Bchl*a*) were found, and the extracted Bchl*a* could be fully reoligomerized.

CD spectra were usually measured on a computerized home-built spectropolarimeter (details will be given elsewhere) and were found to be in very good agreement with measurements done on a Jasco J500C instrument. Ellipticity was calibrated with an aqueous solution of *d*-camphorsulfonic acid at 1 mg/ml (θ_{292} = 0.308°).

Absorbance was measured with computerized Bausch and Lomb (Milton–Roy) Spectronics 1001 and Cary 219 (Varian) spectrophotometers. Fluorescence was measured with a Perkin–Elmer MPF-44A spectrofluorimeter. Atomic absorption was recorded by a Perkin–Elmer 306 spectrometer.

RESULTS

Spectral Forms of Bchl*a* in Fw with no TX-100. Bchl*a* makes two spectral forms in Fw (26): one, termed Bchl-780, has maximum near-IR absorption at 780 nm and the other one, termed Bchl-860, has maximum absorption at 860 nm. The notations [Bchl-780], [Bchl-860], and [Bchla_T] represent the concentration of single molecules of Bchl*a* in the Bchl-780 form, in the Bchl-860 form, and in all forms, respectively.

When [Bchla_T] is $<3 \times 10^{-7}$ M, [Bchl-860] drops to zero (26) and [Bchla_T] = [Bchl-780]. Therefore, to find the absorption of 1 M Bchl-780 in a 1-cm pathlength ($\varepsilon_\lambda^{\text{Bchl-780}}$), we divided the absorption of Bchla_T in Fw by its concentration (Fig. 1).

To find the absorption of 1 M Bchl-860 in a 1-cm pathlength ($\varepsilon_\lambda^{\text{Bchl-860}}$), we introduced a known amount of Bchla_T into Fw and measured its absorption. Then we separated the Bchl-860 by ultracentrifugation at 48,950 × *g* (26) and calculated the concentration of the residual Bchl-780 from its absorption by using $\varepsilon_{780}^{\text{Bchl-780}} = 6.5 \times 10^4$ $M^{-1}\cdot cm^{-1}$. The contribution of Bchl-780 was subtracted from the total absorption and the residual absorption was divided by ([Bchla_T] − [Bchl-780]) to yield $\varepsilon_\lambda^{\text{Bchl-860}}$ (Fig. 1). Once $\varepsilon_\lambda^{\text{Bchl-780}}$ and $\varepsilon_\lambda^{\text{Bchl-860}}$ were obtained we could calculate [Bchl-780] and [Bchl-860] for a given [Bchla_T]. After 20 hr, only 5×10^{-7} M Bchl-860 stayed in the solution, but the spontaneous precipitation was slow enough to allow absorbance and CD (Fig. 2*A*) measurements.

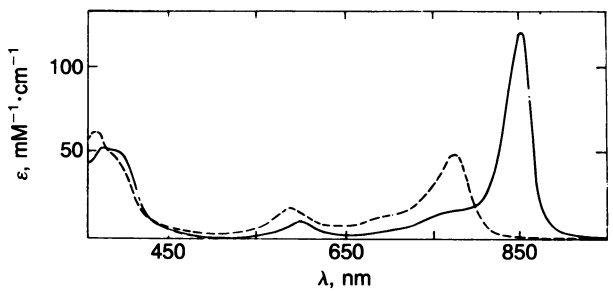

FIG. 1. Absorption of Bchl-860 (—) and Bchl-780 (– – –) in Fw containing no TX-100 or 5×10^{-2} M TX-100, respectively.

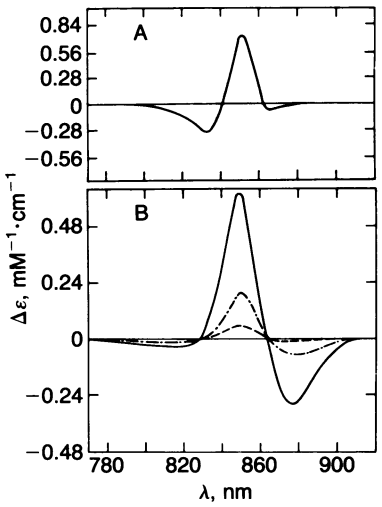

FIG. 2. (*A*) CD spectrum of Bchl-860 Fw. (*B*) CD spectra of Bchl-853 recorded 24 hr after preparation in Fw that contained 5.77 × 10^{-3} M TX-100 and 0.36 × 10^{-6} M Bchl-853 (– – –), 1.5 × 10^{-6} M Bchl-853 (–·–), or 4.15 × 10^{-6} M (—) Bchl-853.

Spectral Forms of Bchl*a* in Fw That Contains Various Amounts of TX-100. The introduction of increased concentrations of TX-100 to Fw solutions that contained about 8 × 10^{-6} M Bchla_T, either before or after the formation of Bchl-860, had the following consequences. (*i*) [Bchl-780] increased with [TX-100] (Fig. 3) according to the equation

$$[\text{Bchl-780}] = B\cdot[\text{TX-100}] + 2.5 \times 10^{-7}\ \text{M}, \qquad [1]$$

where $B = 0.7 \times 10^{-4}$ for [TX-100] < 3×10^{-3} M and $B = 3.2 \times 10^{-4}$ for [TX-100] > 3×10^{-3} M.

(*ii*) There was no change in the lineshapes of the Bchl-780 absorption and CD spectra as [Bchl-780] increased. At sufficiently high [TX-100], Bchla_T converted almost completely into the Bchl-780 form (Fig. 1). [Bchl-780] was then found by Mg^{2+} atomic absorption spectroscopy (26) and used to recalculate $\varepsilon_\lambda^{\text{Bchl-860}}$ in the presence of TX-100 (the same as with no TX-100).

(*iii*) The quantum yield of the Bchl-780 fluorescence (at 793 nm) increased to 0.10, close to the yield of Bchl*a* monomers in methanol (0.12; ref. 36).

(*iv*) The absorption maximum in the near-IR region shifted to 853 nm. Except for some differences in the bandwidth and the slight blue shift of the Q_y transition, the optical absorption of Bchl-860 and Bchl-853 looked the same. We shall use the notation [Bchl-853] for the concentration of Bchl*a* single

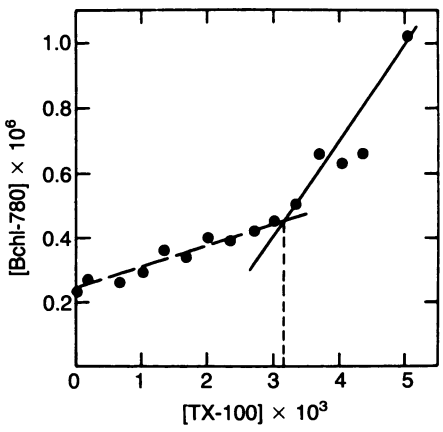

FIG. 3. Dependence of [Bchl-780] on [TX-100] in Fw that contained 8 × 10^{-6} M Bchla_T.

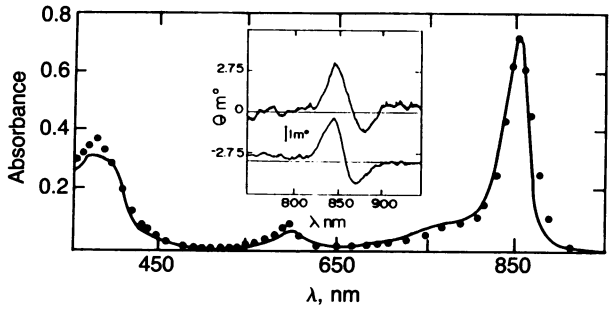

FIG. 4. Optical absorption of Bchl-853 (solid line) and the LHC B850 (●). B850 was extracted as described in ref. 4. (*Inset*) CD spectra of B850 (upper curve) and Bchl-853 (lower curve).

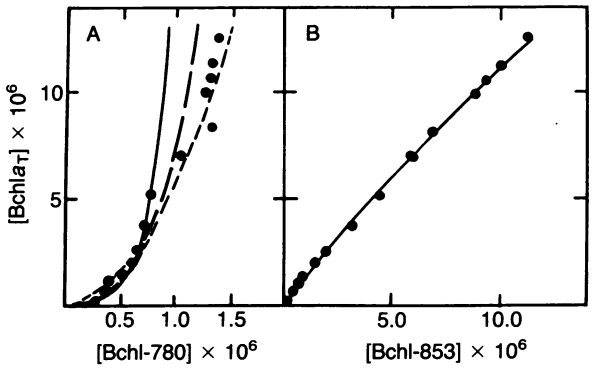

FIG. 5. (*A*) [Bchla_T] as a function of [Bchl-780] in Fw that contained 5.77 × 10^{-3} M TX-100. ●, Experimental values; ---, calculated curve for [Bchl-853] = $\overline{K_2}$[Bchl-780]^2; ———, calculated curve for [Bchl-853] = $\overline{K_3}$[Bchl-780]^3; —, calculated curve for [Bchl-853] = $\overline{K_4}$[Bchl-780]^4. $\overline{K}$ is the average equilibrium constant for the particular reaction order. (*B*) [Bchla_T] as a function of [Bchl-853]. ●, Experimental values; calculated curve for [Bchla_T] = 4.9 × [Bchl-853]^2 + [Bchl-780].

molecules in the new spectral form. The absorption of 1 M Bchl-853 in a 1-cm pathlength ($\varepsilon_\lambda^{\text{Bchl-853}}$) was calculated from the relative change in absorbance at 853 and 780 nm when a small fraction of Bchl-853 was converted to Bchl-780 (e.g., by increasing the [TX-100]). The optical absorption of Bchl-853 (Fig. 4, solid line) is very close to the optical absorption of the LHC B850 (dotted line).

(*v*) The triple-banded CD of Bchl-860 at 860 nm (Fig. 2*A*) was replaced by a doublet with negative and positive extrema at 877 and 850 nm, respectively (Fig. 2*B*). The rotational strength was net positive in the near-IR region and net negative in the UV and visible regions (Table 1).

Spectral Forms in Fw That Contains Various Amounts of Bchl*a* and Fixed Amounts of TX-100. When we held [TX-100] at 5.77 × 10^{-3} M and changed [Bchla_T] the following were observed: (*i*) [Bchl-780] increased (Fig. 5*A*) and could be related to [Bchla_T] by the equation

$$[\text{Bchl}a_T] = 4.90 \times 10^6[\text{Bchl-780}]^2 + [\text{Bchl-780}]. \quad [2]$$

(*ii*) [Bchl-853] was given by

$$[\text{Bchl-853}] = 4.90 \times 10^6[\text{Bchl-780}]^2 \quad [3]$$

for [Bchl*a*] ≤ 10^{-5} M (Fig. 5*B*). At higher values, [Bchl-780] approached an asymptotic value (1.5 × 10^{-6} M) and the 853-nm absorption broadened and shifted toward 860 nm.

(*iii*) The CD in the near-IR region changed from being almost single-banded and positive at low [Bchla_T] values into an almost conservative double-banded CD at high values of [Bchla_T] (Fig. 2*B*). The similarity between the CD lines of Bchl-853 and B850 is illustrated in Fig. 4 *Inset*.

(*iv*) The quantum yield for the fluorescence of Bchl-780 was close to that of Bchl*a* in methanol, up to [Bchla_T] = 0.8 × 10^{-6} M, but decreased at higher values. No fluorescence could be resolved for Bchl-853.

DISCUSSION

Unique geometries of Bchl and bacteriopheophytin dimers have been correlated with their absorption and CD spectra by application of an extended version of the exciton theory (33). Calculation of the geometry of a hypothetical Bchl*a* dimer with the spectral properties of P-860 (26) and B850 (25) led to a structure similar to the one found for P-860 by x-ray crystallography (37, 38). In the proposed geometry the photoexcited singlet states are strongly coupled, and there is

Table 1. Spectroscopic properties of Bchl-780, Bchl-853, the LHC B850 isolated according to ref. 4, and the primary donor P-860 from *Rhodobacter sphaeroides*

	Q_y			Q_x			B_{xy}		
	λ_{max}, nm	Dipole strength, D^2	Rotational strength, D-BM	λ_{max}, nm	Dipole strength, D^2	Rotational strength, D-BM	λ_{max}, nm	Dipole strength, D^2	Rotational strength, D-BM
Bchl-780	780	41.5	+0.05	585	9.0	−0.05	367 392	81 36	+0.05
Bchl-853	853 877	130	+0.6*	595 604	18.0 0.0	−0.0 −0.248	420† 390† 360†	210‡	−0.091 +0.74 −1.57
B850§	852 877	130.0	+0.4*	593 610	20.0 0.0	−0.15*	376	192‡	¶
P-860	860	130	+1.46‖	600	¶	−0.2	¶	¶	¶
Bchla_2 (predicted)	851	117	0.85	595	14.4	+0.73	341 383	4.5 75.2	−3.2 +5.2
	733	0.5	−0.26	604	11.4	−0.97	393 401	134.6 12.9	−1.7 −0.5

The dipole and rotational strengths were calculated as described (5); D, debye; BM, bohr magneton. B_x and B_y were estimated by deconvolution of the Soret band.

*Sum of negative and positive rotations of the particular transition.

†Numbers refer to the extrema of the Soret region.

‡Dipole strength for total Soret band.

§Untreated.

¶Contribution is not yet resolved.

‖At least half due to interaction with the accessory Bchl*a*.

also a coupling of ground states and doubly excited states (33). As a result, the Q_y shifts to about 850 nm, gains oscillator strength, and becomes optically active in a nonconservative way (25, 26, 33). When two such dimers get closer (as in the LHC), their shifted Q_y transitions may be coupled weakly. The coupling may hardly affect the optical absorption spectra but should introduce a significant conservative CD around 850 nm (25). So far we had no supporting evidence for these predictions because none of the *in vivo* compounds could be unambiguously isolated in a dimeric state. However, the strong resemblance of the spectra of Bchl-853, B850, and P-860 (Fig. 4 and Table 1) indicates that the individual components of all forms have similar geometry and may therefore support the theory, provided that Bchl-853 is a dimer. To find the stoichiometry of Bchl-853 we first identified the accompanying compound Bchl-780.

Bchl-780 is probably a Bchl*a* monomer: (*i*) the lineshapes of its absorption and CD spectra do not depend upon its concentration and are typical of Bchl*a* monomers in protic solvents; (*ii*) when no other forms (e.g., Bchl-853 or Bchl-860) are present, it has the normal quantum yield expected for monomers in protic solvents (36); (*iii*) HPLC and TLC of the Bchl*a* that was extracted from the Fw solutions showed no chemical modification (e.g., 10-hydroxy-Bchl*a* formation). Since the concentration of Bchl-780 in the presence of TX-100 exceeds its solubility in pure Fw (value of 2.5×10^{-7} M; ref. 26), it must be solubilized by micelles of TX-100 formed at $>3 \times 10^{-3}$ M TX-100.† The solubilization can be described as

$$\text{Bchl}a + \text{MT} \overset{K_1}{\rightleftharpoons} \text{MT–Bchl}a, \qquad [4]$$

where Bchl*a* represents monomers in free solution, MT represents the TX-100 micelles, and MT–Bchl*a* represents monomers solubilized by the micelles. The concentration of Bchl-780 should be given by

$$[\text{Bchl-780}] = [\text{Bchl}a] + [\text{MT–Bchl}a]. \qquad [5]$$

Since [Bchl*a*] is limited to 3×10^{-7} M, [Bchl-780] should have an asymptotic value given by

$$[\text{Bchl-780}]_\infty = 3 \times 10^{-7}\,(1 + K_1[\text{MT}]). \qquad [6]$$

We found that for [TX-100] $= 5.77 \times 10^{-3}$ M and [Bchla_T] $= 12 \times 10^{-6}$ M, [Bchl-780]$_\infty$ approaches 1.5×10^{-6} M; hence, K_1[MT] = 4. Obviously, as long as [Bchl-780] $< 1.5 \times 10^{-6}$ M, [Bchl*a*] $< 3 \times 10^{-7}$ M, which is the onset for the Bchl-860 formation (26), and the free Fw solution contains only monomers. The quenching of the fluorescence from Bchl-780 that accompanied increased [Bchl-853] could therefore be explained by assuming energy transfer from Bchl-780 to Bchl-853 species that act as energy traps. Hence, the Bchl-853 oligomers must be solubilized within the micelles together with the Bchl-780 monomers and we may write the following set of equations:

$$\begin{gathered}\text{Bchl}a + \text{MT} \overset{K_1}{\rightleftharpoons} \text{MT–Bchl}a \\ \text{MT–Bchl}a + \text{Bchl}a \overset{K_1}{\rightleftharpoons} \text{MT–2Bchl}a \overset{K_2}{\rightleftharpoons} \text{MT–(Bchl}a)_2 \\ \text{MT–(Bchl}a)_n + \textit{Bchla} \overset{K_n}{\rightleftharpoons} \ldots \overset{K_{n+1}}{\rightleftharpoons} \text{MT–(Bchl}a)_{n+1}.\end{gathered} \qquad [7]$$

However, at [Bchla_T] $< 10^{-5}$ M only two spectral forms were observed: Bchl-780 and Bchl-853; hence, the concentration sum of all Bchl*a* monomers equals [Bchl-780]. Combining Eqs. **5**, **6**, and **7** results in

$$[\text{Bchl}a_T] = \text{Bchl-780} + 4\sum_{i=2}^{n} i K_1^{i-1}\{([\text{Bchl-780}]/5)^i \textstyle\prod_i K_i\}. \qquad [8]$$

A comparison of Eqs. **8**, **2**, and **3** shows that $n = 2$ and $K_1K_2 = 3.1 \times 10^7\ \text{M}^{-1}$. Since K_1[MT] = 4 and [MT] $= 5 \times 10^{-7}$ M, $K_1 = 8 \times 10^6\ \text{M}^{-1}$ and $K_2 = 4\ \text{M}^{-1}$.

When [Bchla_T] $> 12 \times 10^{-6}$ M, [Bchl*a*] approaches 3×10^{-7} M and Bchl*a* should form Bchl-860 outside the micelles. We therefore suggest that there are two modes of Bchl*a* oligomerization in Fw containing TX-100. In one mode, micellized Bchls form dimers that have a Q_y transition at 853 nm; in the other mode, free Bchls form large oligomers (26, 41) or micelles (8) that have Q_y transition at 860–865 nm. The onset for the second oligomerization in 5.77×10^{-3} M TX-100 is about 12×10^{-6} M Bchla_T and, therefore, the spectral properties of Bchl-853 should be studied at lower values of [Bchla_T]. For 2×10^{-7} M Bchl-853, most micelles should contain one dimer or monomer since [MT] $\approx 0.5 \times 10^{-6}$ M (A.S., J. Fischer, V.R.-B., unpublished results). Consequently the CD pattern should mainly reflect isolated dimers with the predicted positive Cotton effect at about 852 nm (Q_y transition) and negative Cotton effect at 604 nm (Q_x transition) (Fig. 2*B* and Table 1). The optical absorption and CD of the isolated dimers ([Bchl-853] $\leq 2 \times 10^{-7}$ M) could be best fitted by the geometry shown in Fig. 6, which is slightly different from the proposed geometry of the LHC B850 (25). As [Bchl-853] increases, there should be some micelles populated with several dimers, and dipolar interaction among the shifted Q_y transitions of the trapped dimers should add a conservative contribution to the CD spectrum (Fig. 2*B*, — and –·–). This accounts for the similarity between the CD patterns of Fig. 2 and nonbleached B850 (ref. 16 and Fig. 4) and supports the hypothesis that weak coupling of Bchl dimers may account for the S-shaped CD spectrum of B850 around 850 nm (25).

To account for the similar absorption of the large oligomer (Bchl-860) and the small dimer (Bchl-853), we assume that hydrophobic interactions among the alcoholic residues (42) (Fig. 6*B*) bring the Bchls to within 20–30 Å of one another. At such a distance the absorption spectrum of individual dimers should be hardly affected, but the CD pattern may show dramatic variations (Fig. 2 and ref. 25). Such structures

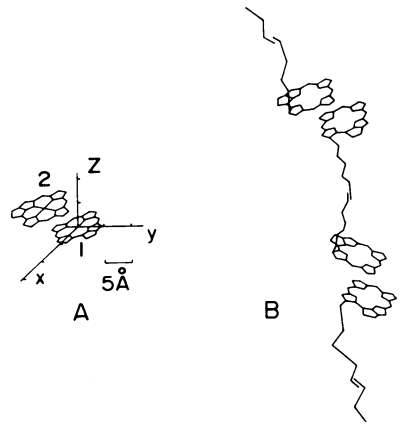

FIG. 6. (*A*) Possible structure for the Bchl-853 dimer. Bchl*a* 1 is centered at the origin; Bchl*a* 2 is at $-0.5x$, $-5.7y$, $+3.5z$. The angles between the transition dipoles are as follows: Q_y2Q_y1, 165°; Q_x2Q_y1, 105°; Q_y2Q_x1, 102°; Q_x2Q_x1, 29°. The angles between the transition dipoles of Bchl*a* 2 and the normal to Bchl*a* 1 are as follows: Q_y2Z1, 80°; Q_x2Z1, 115°. (*B*) Possible oligomerization of Bchl dimers into Bchl-860.

†The reported values for the critical micellar concentration of TX-100 in water range from 3×10^{-4} M (39) to 5×10^{-3} M (40).

can be readily formed in high-dielectric solvents and may be folded to form the very large micelles described by Worcester *et al.* (8). The TX-100 micelle can solubilize the alcoholic residues within its hydrophobic core, thereby breaking the large structures into single pairs.

Two major conclusions can be derived from our study. (*i*) The Q_y shift from 780 to about 850 nm and other spectral properties of Bchl-853, B850, and P-860 are primarily due to strong coupling between ground and excited states within dimers and higher aggregates. (*ii*) The Bchls self-organize into very similar structures in very different environments. This self-organization does not involve the Mg^{2+}–keto interactions traditionally invoked by Katz and co-workers (12) but may be strengthened by interaction of the Mg^{2+} of one molecule with the acetyl group at carbon 2 of the other molecule (J. J. Katz, personal communication). It resembles the dimerization of aromatic side chains within proteins (43–46) and may be due to quadropole–monopole interactions. The Gibbs energy change for such interaction among two phenylalanines can amount to −1 to −2 kcal/mol (44, 46). The corresponding ΔG for the Bchl-780 self-dimerization within the micelles equals −0.9 kcal/mol. Since the x-ray configuration of P-860 and the predicted configuration of B850 are similar to that of Bchl-853, we expect them to have ΔG values in the same order of magnitude and therefore to make a large contribution to the configuration stability of the *in vivo* protein–chromophore matter.

We are grateful to Prof. H. Scheer (Munich), Prof. S. Malkin (Rehovot), and Prof. W. W. Parson (Seattle) for helpful discussions and critical reading of the manuscript. A.S. is a Bat-sheva de Rothschild Fellow and incumbent of the Recanati Career Development Chair. This study was financially supported by the U.S.–Israel Binational Science Foundation (Grant 84-00144).

1. Zuber, H. (1985) *Photochem. Photobiol.* **42,** 821–844.
2. Zuber, H. (1986) *Trends Biochem. Sci.* **11,** 414–419.
3. Cogdell, R. J. & Thornber, J. P. (1980) *FEBS Lett.* **122,** 1–8.
4. Sauer, K. & Austin, L. A. (1978) *Biochemistry* **17,** 2011–2019.
5. Scherz, A. & Parson, W. W. (1984) *Biochim. Biophys. Acta* **766,** 653–665.
6. Thornber, J. P., Cogdell, R. J., Pierson, B. K. & Seftor, R. E. B. (1983) *J. Cell. Biochem.* **23,** 159–169.
7. Ballschmiter, K., Truesdell, K. & Katz, J. J. (1969) *Biochim. Biophys. Acta* **184,** 604–613.
8. Worcester, D. L., Michalsky, T. J. & Katz, J. J. (1986) *Proc. Natl. Acad. Sci. USA* **83,** 3791–3795.
9. Ballschmiter, K. & Katz, J. J. (1972) *Biochim. Biophys. Acta* **256,** 307–327.
10. Krasnovskii, A., Bistrova, M. I. & Umrikhina, A. V. (1977) *Dokl. Akad. Nauk SSSR* **235,** 232–235.
11. Shipman, L. L., Norris, J. R. & Katz, J. J. (1976) *J. Phys. Chem.* **80,** 877–882.
12. Yuen, M. I., Shipman, L. L., Katz, J. J. & Hindman, J. C. (1982) *Photochem. Photobiol.* **36,** 211–282.
13. Katz, J. J., Norris, J. R. & Shipman, L. L. (1977) *Brookhaven Symp. Biol.* **28,** 16–55.
14. Eccles, J. & Honig, B. (1983) *Proc. Natl. Acad. Sci. USA* **80,** 4959–4962.
15. Davis, R. C., Ditson, S. L., Fentiman, A. F. & Pearlstein, R. M. (1981) *J. Am. Chem. Soc.* **103,** 6823–6826.
16. Rafferty, C. N., Bolt, J., Sauer, K. & Clayton, R. K. (1979) *Proc. Natl. Acad. Sci. USA* **76,** 4429–4432.
17. Pearlstein, R. M. & Zuber, H. (1985) in *Antennas and Reaction Centers of Photosynthetic Bacteria*, Springer Series in Chemical Physics, ed. Michel-Beyerle, M. E. (Springer, Berlin), Vol. 42, pp. 53–61.
18. Bolt, J. (1980) Thesis (Univ. of California, Berkeley).
19. Breton, J., Vermeglio, A., Garrigos, M. & Paillotin, G. (1981) *Proceedings of the Fifth International Congress on Photosynthesis*, ed. Akoyunoglou, G. (Balaban International Sciences Services, Philadelphia), Vol. 3, pp. 445–459.
20. Kramer, J. M., Van Grondelle, R., Hunter, C. N., Westerhuis, W. H. J. & Amesz, J. (1984) *Biochim. Biophys. Acta* **765,** 156–165.
21. Zuber, H. (1985) in *Antennas and Reaction Centers of the Photosynthetic Bacteria*, Springer Series in Chemical Physics, ed. Michel-Beyerle, M. E. (Springer, Berlin), Vol. 42, pp. 2–14.
22. Cogdell, R. J. & Valentine, J. (1983) *Photochem. Photobiol.* **38,** 769–772.
23. Theiler, R., Suter, F., Wiemken, V. & Zuber, H. (1984) *Hoppe Seylers Z. Physiol. Chem.* **365,** 703–719.
24. Theiler, R. & Zuber, H. (1984) *Hoppe-Seylers Z. Physiol. Chem.* **365,** 721–729.
25. Scherz, A. & Parson, W. W. (1986) *Photosynth. Res.* **9,** 21–32.
26. Scherz, A., Rosenbach, V. & Malkin, S. (1985) in *Antennas and Reaction Centers of the Photosynthetic Bacteria*, Springer Series in Chemical Physics, ed. Michel-Beyerle, M. E. (Springer, Berlin), Vol. 42, pp. 314–323.
27. Parson, W. W., Warshel, A. & Scherz, A. (1985) in *Antennas and Reaction Centers of the Photosynthetic Bacteria*, Springer Series in Chemical Physics, ed. Michel-Beyerle, M. E. (Springer, Berlin), Vol. 42, pp. 122–130.
28. Warshel, A. & Parson, W. W. (1987) *J. Am. Chem. Soc.* **109,** 6143–6152.
29. Parson, W. W. & Warshel, A. (1987) *J. Am. Chem. Soc.* **109,** 6152–6163.
30. Knapp, E. W., Scherer, P. O. J. & Fischer, S. F. (1986) *Biochim. Biophys. Acta* **852,** 295–305.
31. Scherer, P. O. J. & Fischer, S. F. (1987) *Biochim. Biophys. Acta* **891,** 157–164.
32. Vasinel, H., Amesz, J. & Hoff, A. J. (1986) *Biochim. Biophys. Acta* **852,** 159–168.
33. Scherz, A. & Parson, W. W. (1984) *Biochim. Biophys. Acta* **766,** 665–678.
34. Lubitz, W., Lendzian, F., Plato, M., Mobius, K. & Trankle, E. (1985) in *Antennas and Reaction Centers of the Photosynthetic Bacteria*, Springer Series in Chemical Physics, ed. Michel-Beyerle, M. E. (Springer, Berlin), Vol. 42, pp. 164–173.
35. Haidl, H., Knodlmayr, K., Rudiger, W., Scheer, H. & Schoch, S. (1985) *Z. Naturforsch. C* **40,** 685–692.
36. Connoly, J. S., Samuel, E. B. & Janzen, A. F. (1982) *Photochem. Photobiol.* **36,** 565–574.
37. Allen, J. P., Feher, G., Yeates, T. O., Komia, H. & Rees, D. C. (1987) *Proc. Natl. Acad. Sci. USA* **84,** 5730–5734.
38. Chang, C. H., Tiede, D., Tang, J., Smith, U., Norris, J. & Schiffer, M. (1986) *FEBS Lett.* **205,** 82–86.
39. Yedger, S., Barenholz, Y. & Cooper, V. G. (1974) *Biochim. Biophys. Acta* **363,** 98–111.
40. Kushner, L. M. & Hubbard, W. D. (1954) *J. Phys. Chem.* **58,** 1163–1167.
41. Gottstein, J. & Scheer, H. (1983) *Proc. Natl. Acad. Sci. USA* **80,** 2231–2234.
42. Kratky, C. & Dunitz, J. D. (1977) *J. Mol. Biol.* **113,** 431–442.
43. Burley, S. K. & Petsko, G. A. (1985) *Science* **229,** 23–28.
44. Singh, J. & Thornton, J. M. (1985) *FEBS Lett.* **191,** 1–6.
45. Burley, S. K. & Petsko, G. A. (1986) *J. Am. Chem. Soc.* **86,** 7995–8001.
46. Thomas, K. A., Smith, G. M., Thomas, T. B. & Feldman, R. J. (1982) *Proc. Natl. Acad. Sci. USA* **79,** 4843–4847.